PanTerra Geoconsultants B.V.
Weversbaan 1-3
2352 BZ Leiderdorp
The Netherlands
Tel. +31 71 581 35 05
Fax +31 71 301 08 02
ABNAMRO bank 49 28 54 319
E-mail info@panterra.nl

Prepared for:

TAQA Energy BV
Prinses Margrietlaan 40
2595 BR Den Haag
The Netherlands

Bergen Concession Subsidence Study

Final Report

Volume I: Text, Figures and Tables

Author : Matthias Ziller

Reviewed by: A. van de Weerd and F. de Reuver

Report No. G713-2

May 2010

Intentionally left blank

TABLE OF CONTENTS

1. INTRODUCTION

At the request of TAQA Energy B.V., Den Haag, a surface subsidence study was carried out for the Bergen concession (Onshore Netherlands) which should answer the following question: “What is the total subsidence today due to gas production in the concession and what is the future subsidence that still can be expected?”

The study is an obligatory element in the process of ongoing subsidence monitoring (“Actualisering bodemdalingsprognosis winningsplan Bergen”) by the operator/concession holder.
Regular reporting of subsidence monitoring, as covered in this study, is requested by SodM (Staatstoezicht op de Mijnen/State-supervision of Mines) and will be submitted to SodM.

1.1 Scope of work

The first objective of the study is to make a model which visualises the subsidence up to today as consequence of gasproduction in- and in the surroundings of the concession area. This model should be calibrated to the most recent (i.e 2006) levelling results of the measuring network (i.e. “Meetregister bij het meetplan 2006” winningsvergunning Bergen Alkmaar, pr.nr 17690-159677 dd 15 Aug 2006 /Oranjewoud).
The second objective is to produce a modelled prognosis and visualisation which reflect the additional subsidence hereafter (i.a.w. subsidence after the calibration date in 2006, not including the foregoing subsidence).
The study includes modelled scenarios, both with- and without the gas-storage for the Alkmaar and Bergermeer gasfields.
The area under investigation covers 12 gas reservoirs, 10 of which lie within the Bergen Concession and one lies in the Middelie concession, one straddles the boundary of both concession.
The produced models predict the impact of pressure depletion of the subject gas reservoirs in terms of surface subsidence, based on the theory of poro-elastic compaction and the propagation of this compaction through elastically behaving overburden layers towards the surface.
Modelling was carried out with the use of the TNO developed Software program AEsubs 5.1 Beta and was calibrated against actual surface field subsidence measurements.

2 SUBSIDENCE MODELLING

2.1 Introduction

To understand the cause(s) and development of surface subsidence, the geomechanical behaviour of subsurface rocks is of importance. The main parameters controlling surface subsidence are: rock elasticity parameters, the amount of pore pressure drop, the thickness of the depleting interval and to a lesser extent the elastic properties of the layers below and above the compacting reservoir.

Within the Bergen concession, subsidence has been monitored since the start of production of natural gas. This data has been used to calibrate and verify the model, which has been evaluated in this study.

2.2 Model input and calibration data

Input data was obtained from two sources.

1. TNO, on Taqa's request, provided selected subsidence field data surrounding the Bergermeer field. This data set contains 305 data points. TAQA provided detailed subsurface data, containing field outlines, reservoir thicknesses, depth data as well as data for adjacent aquifers.
2. TAQA provided a dataset of pressure decline and P/Z plots. The Bergermeer Seismicity Study (Muntendam-Bos et al., 2008), provided by TAQA, gave additional information and technical background about subsidence.

Figure 1 (Appendix 5.1.1) gives an overview of all field data and subsidence measurements available for and used in this study. Table 1 lists the fields included in this study and some key parameters.

Table 1: Overview of basic field parameters

Fieldname	Formation	Reservoir Reference Depth [m TVDSS]	Initial Pressure [bar]
Bergen	Buntsandstein	1430.0	143.0
Boekel	Buntsandstein	1576.0	168.0
Alkmaar	Zechstein	2026.0	195.8
Schermer	Zechstein	2113.0	220.6
Schermer-Zuid	Zechstein	2132.0	218.3
Starnmeer	Zechstein	2014.0	205.7
Bergen	Rotliegend	2108.5	218.0
Bergermeer	Rotliegend	2197.5	227.8
Groet	Rotliegend	2185.5	229.3
Groet-Oost	Rotliegend	2250.5	234.6
Schermer	Rotliegend	2428.0	253.3
Westbeemster	Rotliegend	2572.0	290.0

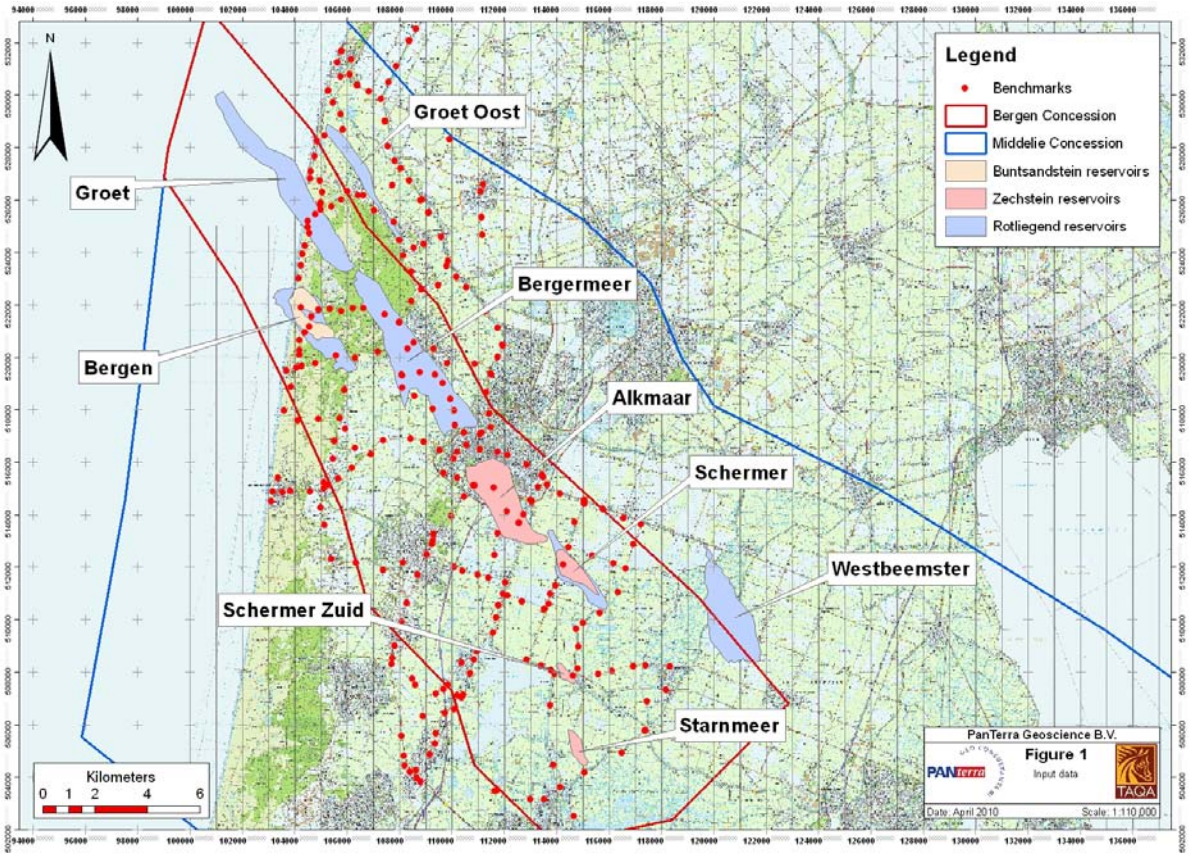

Figure 1 : Field outlines and subsidence measurement points included in this study

The subsidence measurements provided to Panterra include 56 measurements dating back to 1972 and 123 measurements dating back to 1980/1981. Locations of measurements (Benchmarks) from 2006 overlap with 46 points from 1972 and 101 data points from 1980/1981. The dataset contained 76 points with measurements between 1972 and 1980/81. Those three datasets have been used to calibrate and validate the present subsidence model. Several of the provided benchmarks have not been levelled in the time spans analysed and were therefore not used.

A maximum of approximately 10.5 cm subsidence occurred since 1972. Of this 10.5 cm approximately 9.2 cm subsidence occurred since 1980. The maximum subsidence observed occurs in the triangle between the fields Bergermeer, Groet and Bergen fields, of which the first two produce from the Rotliegend and the last one from both Bunter and Rotliegend reservoir sands. Interaction of production and depletion of these four fields resulted in the maximum subsidence observed thus far in this area.

2.2.1 Uncertainty analysis of provided benchmarks

Every benchmark measurement is subject to errors, which can be divided into two categories: Drift and random errors / noise.

Drift

Benchmark stability information used to be provided by the DID (Rijkswaterstaat Data-ICT-Dienst), but is no longer available from their database. According to Houtenbos (2008), 93%

of the benchmarks fall into the highest stability class. The highest stability benchmarks have a drift between 0 and 0.50 mm/a. The average is therefore 0.25 mm.
For a benchmark installed in 1972 and last measured in 2006, this gives an error of 34 * 0.25 mm/a = 8.5 mm. The error for a benchmark installed in 1981 and last levelled in 2006 leads to an error of 25 * 0.25 mm/a = 6.25 mm.

Random Error / Noise
Each benchmark has an error that depends on the distance between the reference benchmark and the benchmark itself. The distance should be measured along paved roads and is different for every benchmark. The random error is calculated using Equation 1:

$$E_R = 1 * \sqrt{L}$$

Equation 1: Random error equation; with E_R being the random error and L being the distance from the reference point in km

To simplify matters, L was chosen to be 10 km, which is a good approximation.

The total error for a benchmark measurement is the root mean square of the annual plus the random error (Equation 2).

$$E_T = \sqrt{E_D{}^2 + E_R{}^2}$$

Equation 2: Total error equation; with E_T being the Total, E_D being the Drift and E_R being the Random error

This results in two average errors for the three time spans used in this study. These values are summarized in Table 2.

Table 2: Errors of benchmark measurements according to time span

Time Span	Drift	Random Error	Total Error
1972 – 1980/81	2.25 mm	3.2 mm	3.9 mm
1972 – 2006	8.50 mm	3.2 mm	9.1 mm
1980/81 - 2006	6.25 mm	3.2 mm	7.0 mm

After evaluation of all benchmarks, one area showed additional subsidence that is independent from actual gas production. The observed benchmarks 19B238, 19B239, 19B240 and 19B281 are located North of Alkmaar, along the road N9. These benchmarks have been associated with an independent subsidence bowl in the area of the water treatment facility Geestmerambacht as remarked by Houtenbos (2008). They have been therefore excluded from the analysis.

2.2.2 Determination of the formation thickness input parameter for subsidence modelling

The subsidence modelling process assumes a layered model for the overburden as input, with constant formation depths and thicknesses across the whole area of interest. To achieve this, both the actual minimum and maximum formation thicknesses have been taken into account

to determine an average layer thickness, which best honours reality. Model thickness inputs are listed in Table 3, minimum and maximum formation thicknesses are taken from Muntendam-Bos et al., 2008. Departures from calculated averages are due to model constraints (i.e. constant formation depths and thickness).

Where possible, depths of reservoirs have been left unchanged, as a result the thickness had to be adapted in order to fit all reservoirs into a single formation layer. Rotliegend reservoirs in the area occur at depths ranging from 2108 m to 2572 m. In order to fit all Rotliegend reservoirs into a single AEsubs model layer this layer had to be assigned a thickness of 670 m (i.e. difference between top of the shallowest and bottom of the deepest reservoir). The Rotliegend layer thickness is used for the elasticity model only, while the actual reservoir thickness of the depleting intervals is used in the AEsubs calculations. Since there are no depleting reservoirs below the Rotliegend, the exaggerated thickness for this layer was put in to accommodate certain model restrictions in the software and does not influence the calculated subsidence at the surface.
For the model a grid cell-size of 100 m by 100 m has been used.

Table 3 : Layered model thicknesses

Interval	Min. Thickness [m]	Max. Thickness [m]	Avg. Thickness [m]	Model Thickness [m]
Tertiary (Noordzee Grp)	791	877	834	838
Holland + Vlieland	191	675	433	412
Keuper + Bunter	75	815	445	400
Main Claystone	38	441	240	100
Zechstein	0	596	298	330
Slochteren	164	415	290	670

2.3 Subsidence prediction from reservoir compaction

When the reservoir pressure decreases due to gas production, the reservoir itself compacts. Prior to the start of gas production, the reservoir will be in an equilibrium in-situ stress state with a given effective stress-state. However, the pressure drop caused by the withdrawal of gas causes the effective stress to increase. This induces the reservoir rock to compact until a new equilibrium is reached. Due to the elastic coupling between the reservoir and the surrounding rock, the compaction in the reservoir is transferred to the surface almost instantaneously, which results in surface subsidence. However, because the surface rocks are elastic, the subsidence bowl extends over a larger area than the compacting reservoir. The radius of the area affected by subsidence is roughly the same as the depth of the reservoir below the surface (Muntendam-Bos et al., 2008).
As requested by TAQA, the linear, semi-analytic approach designed by Fokker and Orlic, (2006) to account for layering when modelling the relation between reservoir compaction and surface subsidence, was used. This model is the basis for the subsidence calculation software AEsubs, developed by TNO and used in this study (AEsubs 5.1 beta).

2.4 Elasticity parameters

The theory of elasticity holds that no significant damage or alteration of the rock results from the applied stress and assumes that stress and strain are linearly proportional and fully reversible. The material properties known as Young's modulus and Poisson's ratio (E and v, respectively) determine the elastic behaviour of the subsurface. The Young's modulus is the stiffness of a rock in unconfined uni-axial compression, while the Poisson's ratio is the ratio of lateral expansion to axial shortening.

The parameters listed in Table 4 have been derived from well logs and literature (Muntendam-Bos et al., 2008) by TNO. The input parameters have been validated by the outcome of the modelling results shown in Figure 3 (see paragraph 2.6).

Table 4 : Comparison of elasticity parameters: range and parameter values as used for modelling (after Muntendam-Bos et. al., 2008)

Geological Unit	Range Young's modulus [GPa]	Range Poisson ratio [-]	Used Young's modulus [GPa]	Used Poisson ratio [-]	Depth Formation Top [m]
Tertiary rocks	0.1-1	0.29-0.38	1	0.33	0
Vlieland Shales & Holland Marls	1-15	0.23-0.24	10	0.23	838
Muschelkalk, Bunter & Keuper	5-35	0.24-0.3	25	0.26	1250
Main Claystone	15-35	0.25-0.3	30	0.28	1650
Zechstein Formation	20-50	0.25-0.3	40	0.28	1750
Rotliegend Slochteren Sandstone	10-26	0.1-0.25	25	0.18	2080
Carboniferous	30	0.25	30	0.25	2750

2.4.1 Sensitivity of subsidence to subsurface elasticity parameters

Elasticity parameters have a direct impact on surface subsidence and the lateral extend of the subsidence bowl. To give an idea of maximum impact on subsidence values due to the choice of parameters, the Bergermeer subsidence has been modelled twice, with minimum and maximum values according to Table 4. Both, TNO (Muntendam-Bos et al.) and this study came to a difference of 2.6 cm in depth at the most.

The values of the input parameters, used in this study, are considered to be realistic, as the calculated displacement at surface is in line with the survey values (see section 2.2) for the integrated model. Figure 3 shows the nucleus displacement at surface for the used subsurface model. Paragraph 2.6 gives additional information on verification and calibration of the used values.

2.5 Reservoir depth adjustments

Some reservoir depth values had to be adjusted to honour the layer model. As the Rotliegend aquifers and reservoirs contribute most to total subsidence, the depths of all but one (Bergen) Rotliegend reservoirs have been left un-adjusted. None of the Buntsandstein reservoirs

required a depth adjustment. However, due to the large variation in both the thickness and distribution of the Zechstein, all Zechstein reservoirs had to be depth-adjusted to fit into the model.

Table 5 : Comparison of actual and modelled depth per field

Field name	Formation	Reservoir Reference Depth [m TVDSS]	Modelled Reservoir Depth [m TVDSS]	Difference [m]	Thickness [m]
Bergen	Buntsandstein	1430.0	1430.0	0.0	67
Boekel	Buntsandstein	1576.0	n/a*	n/a*	38
Alkmaar	Zechstein	2026.0	1906.0	120.0	43
Schermer	Zechstein	2113.0	1993.0	120.0	38
Schermer-Zuid	Zechstein	2132.0	1953.0	179.0	38
Starnmeer	Zechstein	2014.0	1953.0	61.0	38
Bergen	Rotliegend	2108.5	2228.5	120.0	263
Bergermeer	Rotliegend	2197.5	2197.5	0.0	235
Groet	Rotliegend	2185.5	2185.5	0.0	270
Groet-Oost	Rotliegend	2250.5	2250.5	0.0	270
Schermer	Rotliegend	2428.0	2428.0	0.0	206
Westbeemster	Rotliegend	2572.0	2572.0	0.0	181

*field Boekel not included in final modeling, see chapter 2.7.

A second reason for depth-shifting of the reservoirs is the modelling assumption that the reservoirs should not be placed too close to an interface of two separate layers , as this would cause the AEsubs program to produce incorrect results. Table 5 shows the differences in actual depth and depth values used in the model. Thickness includes reservoir and aquifer height.

The sensitivity of Zechstein thickness has been tested by running a maximum and a minimum thickness model. According to Table 3, the Zechstein thickness has been modified. The difference between the model using no Zechstein layer and a model with 600 m Zechstein thickness is 1 mm of subsidence at surface.

Modelling of the Bergen Rotliegend field indicates a maximum impact of 0.3 cm reduction of subsidence in the centre of the subsidence bowl due to these depth adjustments in the model. Figure 2 shows the modelled depths of the reservoirs (dots on the Y-axis), combined with the used viscosity and E-moduli values for each layer (the layer interfaces correspond to the depths at which parameters values change).

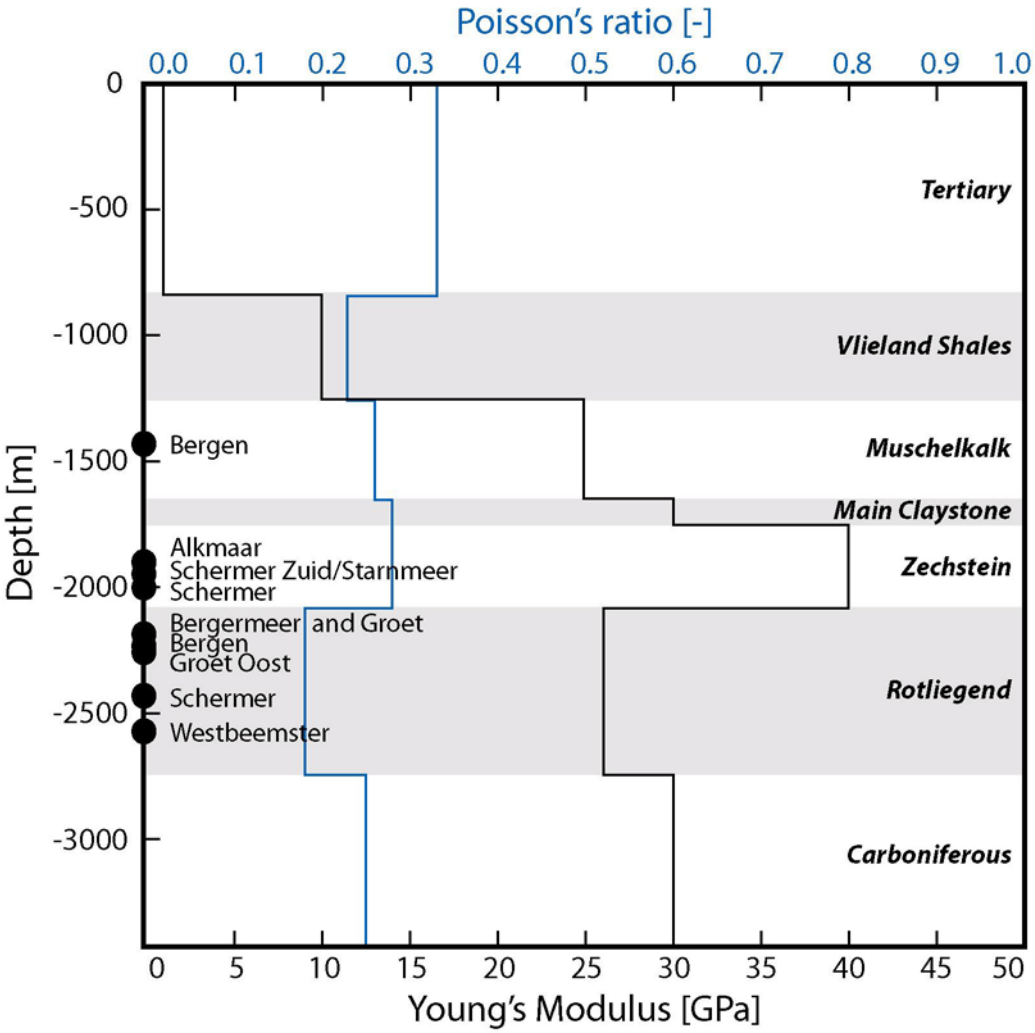

Figure 2 : Overview of used reservoir depths and elasticity parameters

2.6 Model verification

Figure 3 shows a plot of calculated (subsidence) nucleus displacement at surface for each reservoir considered in the model. Using the elasticity values from Table 4, and depth adjustments as described in paragraph 2.5, it shows low divergence of the subsidence curves at the surface (i.e. using wrong parameters results in curves not meeting at the surface profile. This, together with the observations that modelled subsidence bowls and survey data show a good fit (see chapter 3), gives credence to the used model.

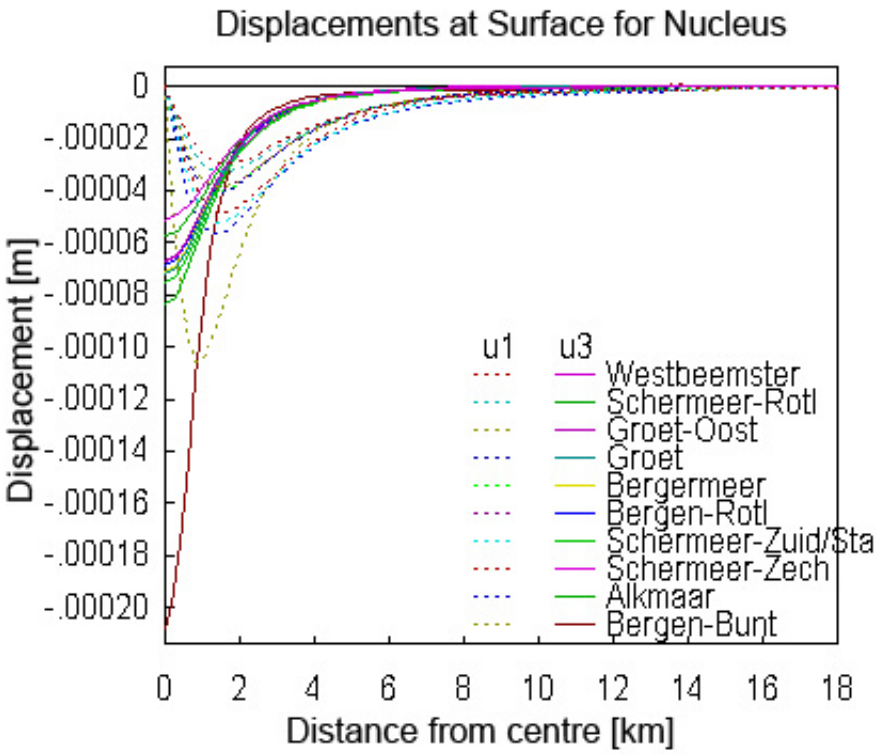

Figure 3 : Plot of Displacement for Nucleus in used model

2.7 Procedure

Twelve reservoirs were involved in the subsidence modelling. Compaction of the reservoirs due to pressure depletion is not restricted to the gas reservoirs alone. It is equally important in the connected aquifers as the pressure drop is transmitted to the aquifers. Aquifers are assumed to be static and of limited aerial extent as no proof of active water drive that could maintain reservoir pressure was found. TAQA provide x,y,z data points (100m spacing) for all of the reservoirs and connected aquifers, with corresponding reservoir thickness. Generally, it was assumed that the connected aquifers extend up to the bounding faults nearest to the gas reservoirs. For the modelling software, which uses grid cell volumes, the z-values were multiplied by the cell dimension (100x100m) to calculate the cell volumes and multiplied by the pressure depletion values for each of the reservoir/aquifers.
The used subsidence modelling program, AEsubs, which was developed by TNO, can handle a maximum of ten different reservoir/aquifer layers in a single modelling run. Each reservoir was allocated a compaction coefficient and a pressure depletion value. To include all reservoirs within the Bergen concession into a single model, some reservoirs had to be joined. Merging two reservoirs requires both reservoirs to have equal thickness, as well as an identical pressure depletion history and compaction coefficients. The number of twelve reservoirs in the area of interest had to be reduced to ten in order to fit into the software model. This was achieved by merging two reservoirs with similar properties and excluding the Boekel field, which could safely be excluded due to its minor size and therefore minimal impact on compaction. Fields Schermer Zuid and Starnmeer that are both of Zechstein age have been merged and treated as one reservoir. The extend of connected Rotliegend aquifers is uncertain as only major bounding faults are visible on seismic. Smaller faults are invisible due to

seismic resolution at this depth. Nonetheless the invisible faults can and are proven to seal different compartments effectively.

2.7.1 Model constraints and properties

It has been established empirically that the ratio of gas reservoir volume versus the volume of the underlying aquifer determines whether a system has active water drive or not. If the volume of the aquifer is less than 10 times the volume of the gas reservoir, water influx during depletion of the gas reservoir (as a result of aquifer water expansion) is expected to be negligible. The P/Z plots of the fields incorporated in study do not show any indication for active water drive, validating the assumption of limited aquifer sizes.
An additional control is provided by the comparison of modelled compaction volumes and gas initially in place (GIIP) volumes. The compaction volume cannot be larger than the volume of extracted gas at reservoir conditions.
The used model keeps the aquifer-reservoir volumes constant in all Rotliegend fields.

2.7.2 Analysis of compaction trends

Non-linear compaction is observed for many of the Rotliegend reservoirs in the study. In this study this behaviour has been approximated using a bi-linear compaction approach. For reservoirs with a near hydrostatic reservoir gas pressure the width of the transition zone observed elsewhere is generally 40 – 50 % of the initial gas pressure. Similar effects are seen for the reservoirs in this study. Therefore cumulative production was plotted against cumulative subsidence (Figure 4) measured at selected benchmarks (Table 6) on top of producing Rotliegend fields. The values in Figure 4 were normalized to make several fields comparable. Normalization was carried out by division of production and subsidence data by the respective 2006 values.

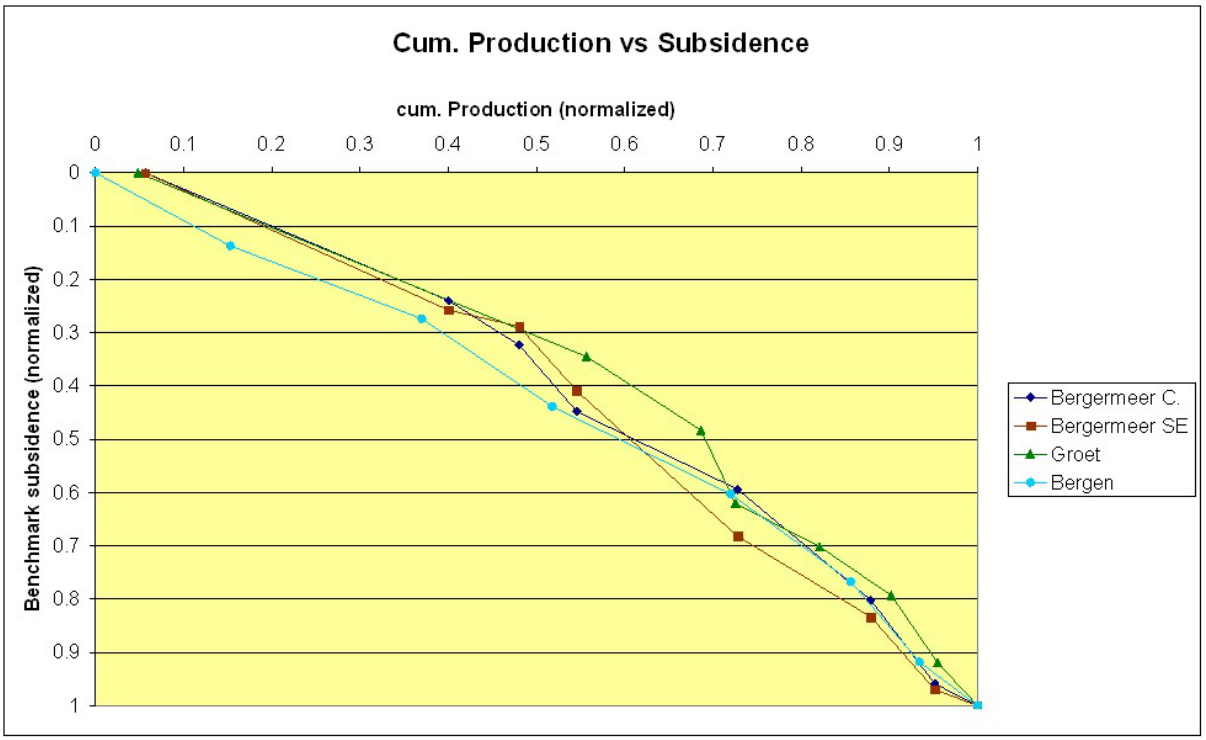

Figure 4: Normalized cumulative production versus normalized subsidence

Break-points are observable, but they are not clearly related to distinct production volumes / pressure declines. This is due to the long intervals between different levelling campaigns, which result in only a small number of points for which the comparison of production and subsidence can be performed.

In order to handle the bilinear compaction, two time spans have been modelled to represent the different compaction coefficients. Evaluating the pressure decline curves it is noticeable that the largest Rotliegend fields, which have the biggest influence on actual subsidence, pass the 30% pressure depletion event around 1980/81. Therefore the time span from 1972 to 1980/81 was chosen to calibrate the first, lower compaction phase. The time span from 1980/81 till 2006 was used to calibrate the subsidence occurring during the second phase.

Table 6: Selected benchmarks above Rotliegend fields

Field	Benchmark
Bergermeer Centre	19A016
Bergermeer South East	19B174
Groet	14C112
Bergen	19A101

2.7.3 Compaction coefficient distribution

Figure 4 reveals different compaction trends within the Bergermeer field, where the compaction increases more in the Southeast after reaching the 30% pressure decline break-point while the increases in the center of the field is lower. This is thought to be due to different gas column heights in the area. To compensate for the gas column height, compaction coefficients were increased in relation to the gas cap thickness. The compaction factor was modified using a five step model, in which the highest increase is a multiplicator of 1.8, resulting in a maximum compaction factor of about 0.65E-5 1/bar, as used by Muntendam-Bos (2008). Areas with a thin gas cap where not altered, resulting in multiplicator of 1. Figure 5 shows the multiplicator distribution for Rotliegend reservoirs within the study area.

To match observed and measured subsidence, the time span from 1972 – 1980/81 did not use increased compaction coefficients over the gas caps (chapter 2.7.2) and a constant compaction coefficient of 0.35*10-5 1/bar. The second time span from 1980/81 – 2006 uses the bilinear compaction model with higher compaction coefficients and a slightly increased compaction coefficient of 0.38*10-5 1/bar. Calculated subsidence bowls were added in order to create the full time span (1972 – 2006) model and compared with benchmarks readings over the same time interval.
Zechstein and Buntsandstein reservoirs use a constant coefficient of 0.35*10-5 1/bar throughout both time spans, which was found to be matching with the observed subsidence measurements. Applied compaction coefficients are summarized in Table 7.

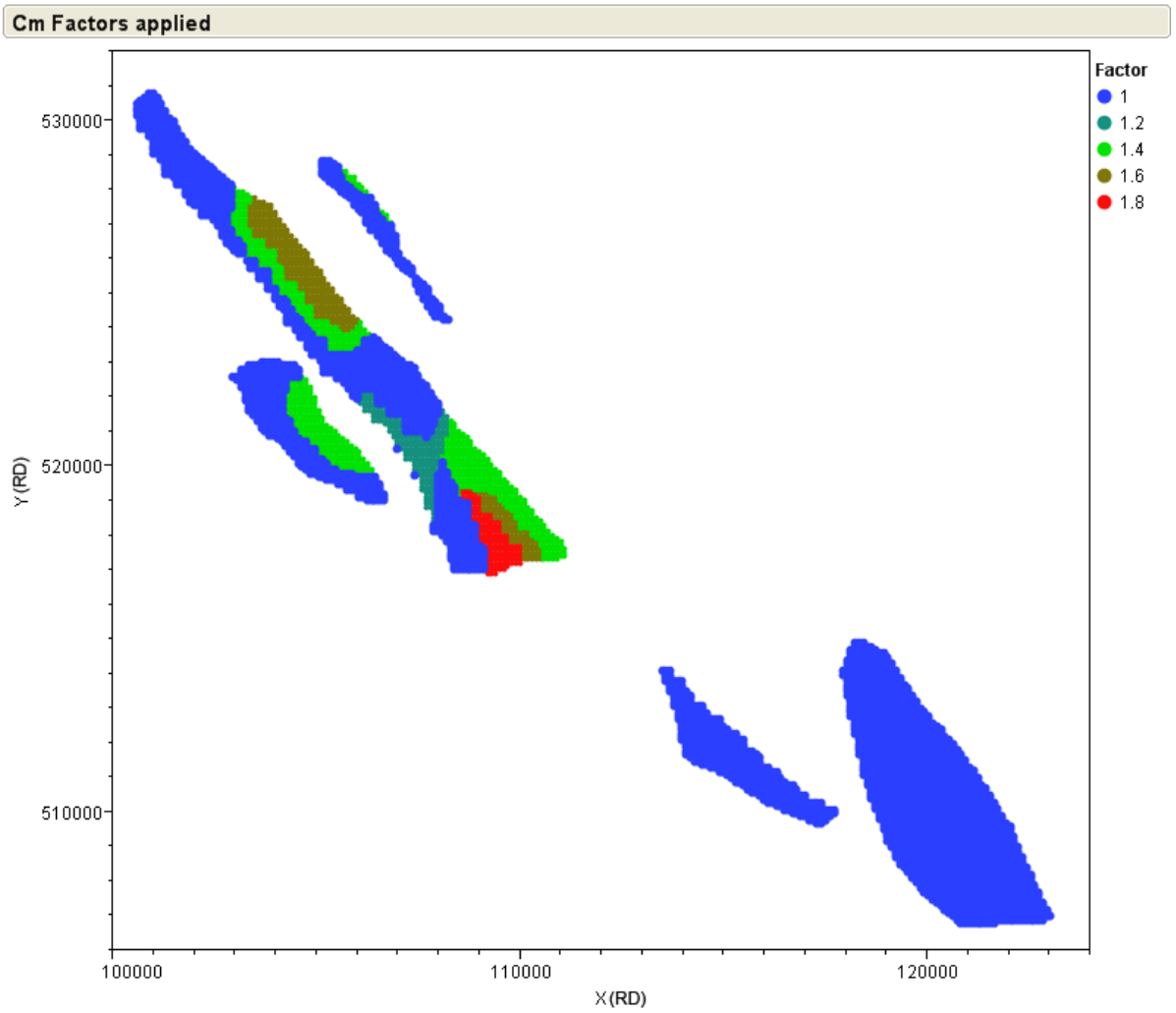

Figure 5: Distribution compaction coefficient multiplicators in the study area

2.7.4 Application of Net to Gross ratios

When including the total aquifer thickness, the model does not take into account formation heterogeneity. Heterogeneity will result in reduced compaction thickness, as only ideally behaving formation sections will contribute with a maximum amount to compaction. For example, intervals of shale will not contribute to compaction, as they are already highly compacted. Areas which are highly cemented, like the Weissliegend layers in the Rotliegend will show limited compaction as well. To account for this aspect, a net to gross ratio was applied. This ratio describes how much of the whole formation will contribute to the compaction. Setting the ratios, several aspects have been taken into account. The Buntsandstein formation is known to contain relatively thick shale intervals, which are laterally quite variable. Zechstein carbonate reservoirs are known to be often affected by invasion and cementation. Rotliegend reservoirs are known to be relatively clean and homogenous. Nonetheless thick, well cemented Weissliegend layers are known to occur in the area of interest. Additionally localized shale layers are also known to occur in the Rotliegend, and should be taken into account. Table 7 gives an overview of each model parameters used, including net/gross ratios.

Table 7: Model parameters

Formation	Time span 1972 – 1980/81	1980/81 – 2006
Compaction coefficients:		
Buntsandstein	$0.35*10^{-5}$ bar^{-1}	$0.35*10^{-5}$ bar^{-1}
Zechstein	$0.35*10^{-5}$ bar^{-1}	$0.35*10^{-5}$ bar^{-1}
Rotliegend	$0.35*10^{-5}$ bar^{-1}	$0.38*10^{-5}$ to $0.65*10^{-5}$ bar^{-1}
Net/Gross ratios:		
Buntsandstein	0.80 -/-	0.80 -/-
Zechstein	0.80 -/-	0.80 -/-
Rotliegend	0.80 -/-	0.80 -/-

2.7.5 Reservoir pressure depletion

All models, have been calibrated and calculated on the basis of reservoir pressure depletion datasets, provided by TAQA. Two sets of subsidence data points have been extracted from the original dataset. The model used measurements from the 1972 to 1980/81 period and data from 1980/1981 to 2006 period to calculate subsidence as a result of pressure decline. The model subsidence predictions that were based on those input pressure measurements were compared with the actual subsidence data as measured in the field measurements over the same time spans. Table 8 gives an overview of the input datasets used.

Table 8: Model pressure input data

Fieldname	Initial Pressure 1972 [bar]	Pressure 1980/1981 [bar]	Pressure 2006 [bar]	Pressure depletion 1972 – 1980/81 [bar]	Pressure depletion 1980/81 – 2006 [bar]	Pressure depletion 1972 – 2006 [bar]
Bergen	143.00	143.00*	75.30	0	67.00	67.70
Alkmaar	195.80	181.20	190.00	14.6	-8.80	5.80
Schermer	220.60	220.60*	50.00	0	170.60	170.60
Schermer-Zuid - Starnmeer	212.00	212.00*	147.00	0	65.00	65.00
Bergen	218.00	182.35	14.60	35.65	167.85	203.40
Bergermeer	227.80	146.80	9.30	81	137.50	218.50
Groet	229.30	124.70	30.00	104.6	94.70	199.30
Groet-Oost	234.60	234.60*	214.30	0	20.30	20.30
Schermer	253.30	234.10*	62.70	19.2	171.40	190.60
Westbeemster	290.00	290.00*	290.00	0	0.00	0.00

* Initial pressure

3 RESULTS

3.1 Modeling results

Comparing the calculated subsidence bowls with the field measurement for each of the modelled time spans shows a good correlation. To assess the fit of modelled and measured data, different methods were used:

- Benchmarks with values covering the modelled time spans (1972 – 1980/81, 1980/81 – 2006 and 1972 – 2006) were selected to evaluate the fit at distinct points.
- Calculated contours from Benchmark data were compared to modelled contours to assess the spatial fit.
- Several cross sections were constructed to investigate the fit with respect of the shape of the modelled subsidence bowl.
- Time series at selected Benchmarks were constructed and evaluated to control the fit over time.

The maximum calculated subsidence in the centre of the subsidence bowl is displayed in Table 9. To provide a quantitative measure, the maximum-recorded subsidence from benchmarks is shown as well. The location of the subsidence bowl centre is different for both time spans modelled. Therefore both maximums do not add up to the full time span value.

Table 9: Maximum subsidence measured and calculated per modelled time span

	1972 – 1980/81	1980/81 – 2006	1972 – 2006
Modelled	2.8 cm	8.5 cm	10.5 cm
Benchmark	5.0 cm	9.8 cm	10.4 cm

Observed fits are discussed in the following chapters.

3.1.1 Fit at benchmark locations and spatial fit for the time span 1972 – 1980/81

The time span from 1972 till 1980/81 was calibrated using 76 benchmarks. Appendix 5.1.2 shows the modelled contours in relation to the observed subsidence at each benchmark. It is observable that the model contours fit well to the measured data. To achieve a better impression of the fit, the discrete benchmark values have been contoured to create a spatial distribution. Figure 6 shows an overlay of modelled contours (thick contours) and contours calculated from benchmark values. It is evident that the spatial distribution shows a good fit.

The spatial and local fit for this short time span has relatively high uncertainty. Only two levelling campaigns (1972 and 1980/81) were taken into account and the measured subsidence is not very large. As a result random errors (see chapter 2.2.1) have a higher influence on the reliability of the measured subsidence. The additional subsidence bowl, as discussed in chapter 2.2.1, influences local benchmarks as well, and makes benchmarks in this area less reliable.

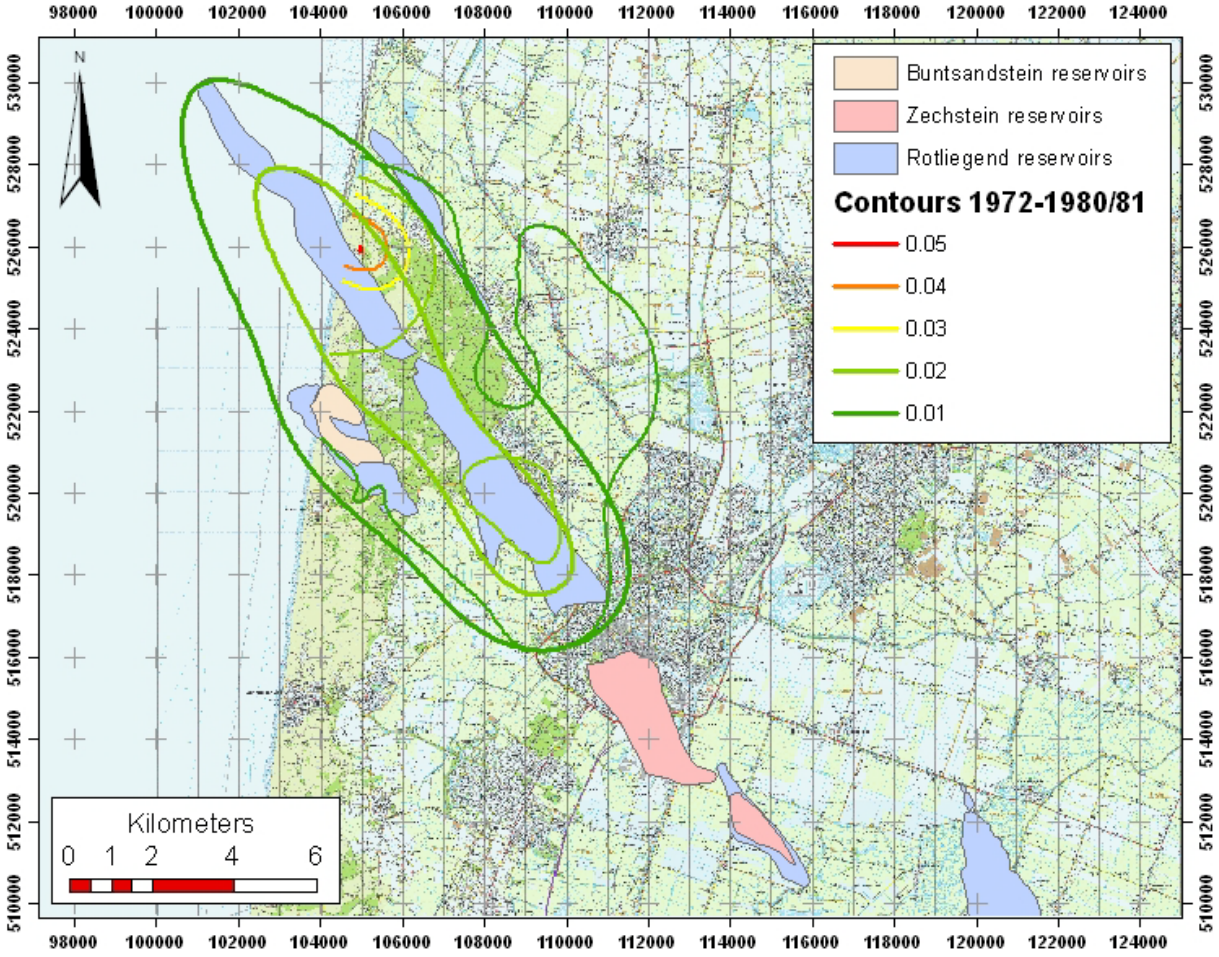

Figure 6: Comparison of benchmarks and model from the time span 1972 - 1980/81. The modelled subsidence is plotted with thick contours, while the benchmark contours are plotted thin.

3.1.2 Fit at benchmark locations and spatial fit for the time span 1980/81 – 2006

The time span from 1980/81 till 2006 was calibrated using 101 benchmarks. Appendix 5.1.3 shows the modelled contours in relation to the observed subsidence at each benchmark. The model values fit well to observed distinct subsidence measurements. The contoured benchmarks show a good spatial fit with modelled subsidence as well. Figure 7 shows an overlay of modelled contours (thick contours) and contours calculated from benchmark values.

The benchmarks showing additional subsidence in the Northern West of the Bergermeer field (chapter 2.2.1) have not been included to calculated contours from benchmarks. However, they were plotted to show the complete dataset.

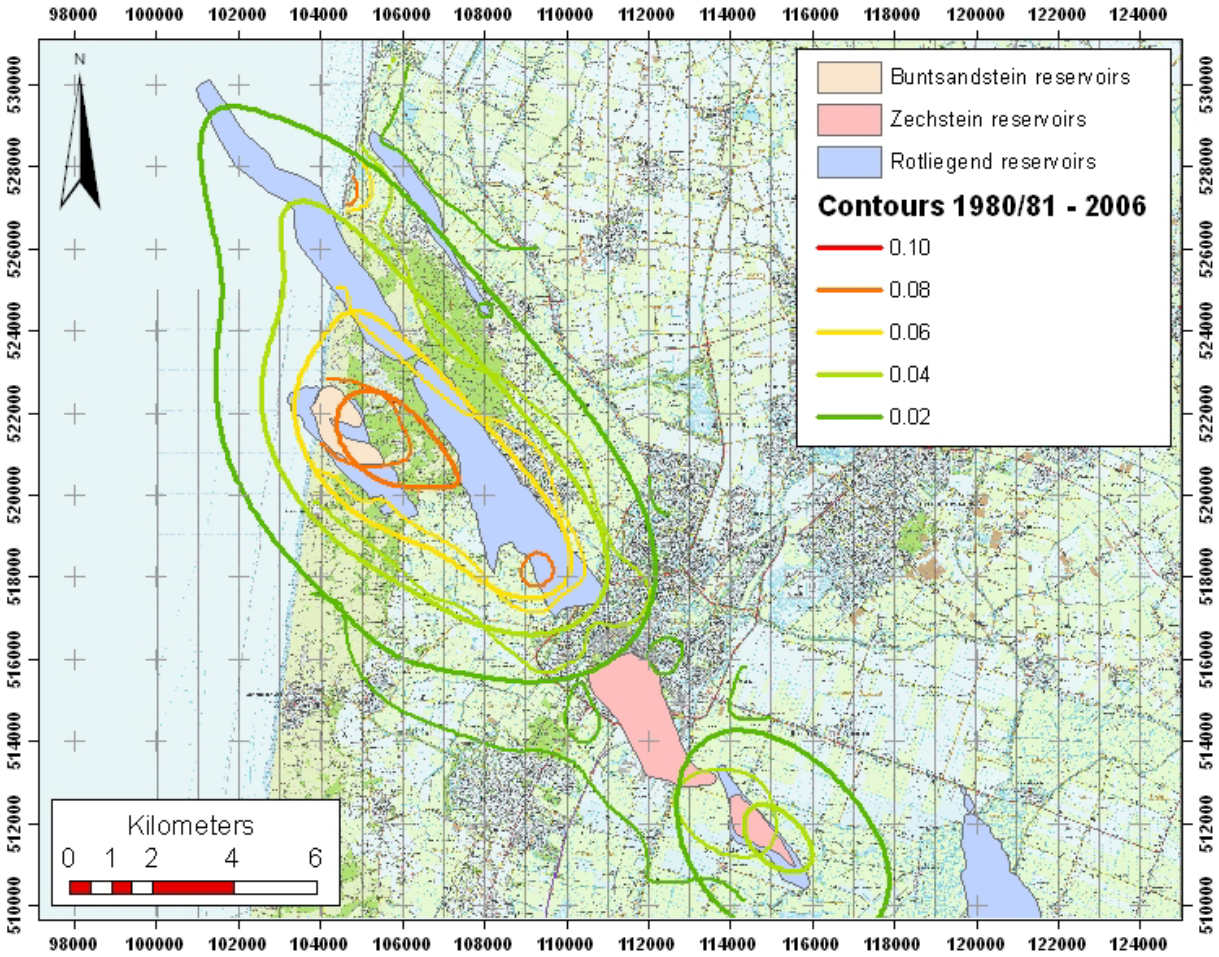

Figure 7: Comparison of benchmarks and model from the time span 1980/81 – 2006. The modelled subsidence is plotted with thick contours, while the benchmark contours are plotted thin.

3.1.3 Fit at benchmark locations and spatial fit for the time span 1972 – 2006

The time span from 1972 till 2006 was calibrated using 46 benchmarks. Appendix 5.1.4 shows the modelled contours in relation to the observed subsidence at each benchmark. The model values fit well to observed distinct subsidence measurements. The contoured benchmarks show a good spatial fit with modelled subsidence as well. Figure 8 shows an overlay of modelled contours (thick contours) and contours calculated from benchmark values.

This time span has the least control by actual benchmark measurements. The minor misfit of contoured benchmark and modelled subsidence in the Southern East section of the Bergermeer field is believed to be due to poor data coverage. Both input time spans, 1972 – 1980/81 and 1980/81 – 2006, show a good fit in this area. Therefore the model is considered to be fitting well, as actual field measurements affirm the fit at distinct points.

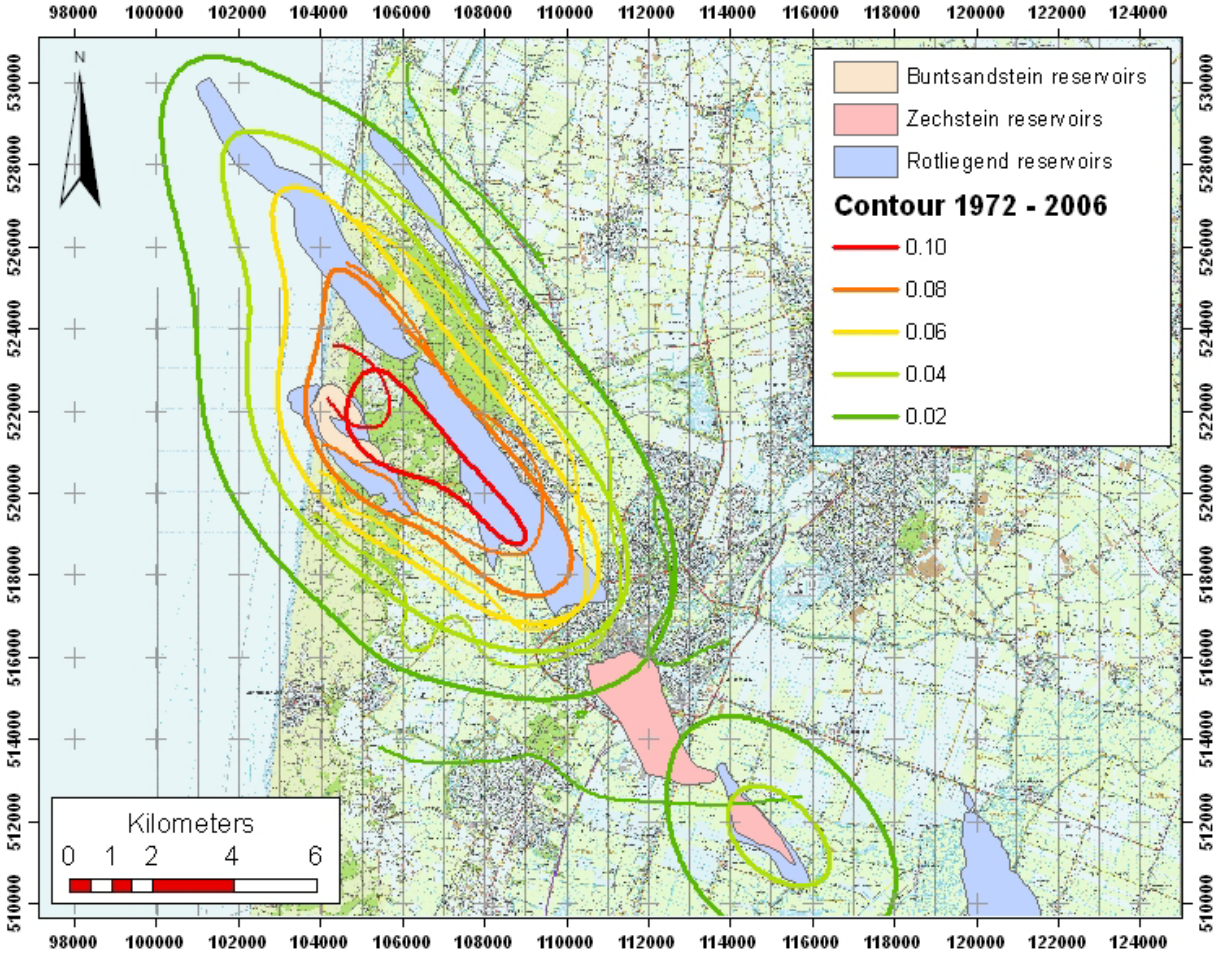

Figure 8: Comparison of benchmarks and model from the time span 1972 – 2006. The modelled subsidence is plotted with thick contours, while the benchmark contours are plotted thin.

3.1.4 Cross sections

In order to evaluate the observed fit in more detail, four cross sections were constructed. Three sections are perpendicular to the long axis of the subsidence bowl (Sections I, II and III), while one section (IV) is perpendicular to the first three sections. Figure 9 shows the location and the cross sections and the benchmarks that lie on it. Two time spans (1972 – 2006 and 1980/81 – 2006) are shown in the resulting cross sections that are presented in Figure 10, Figure 11, Figure 12 and Figure 13. Both time spans are overlain by its respective benchmarks, where available. The benchmarks show an error bar, whose derivation is discussed in chapter 2.2.1.

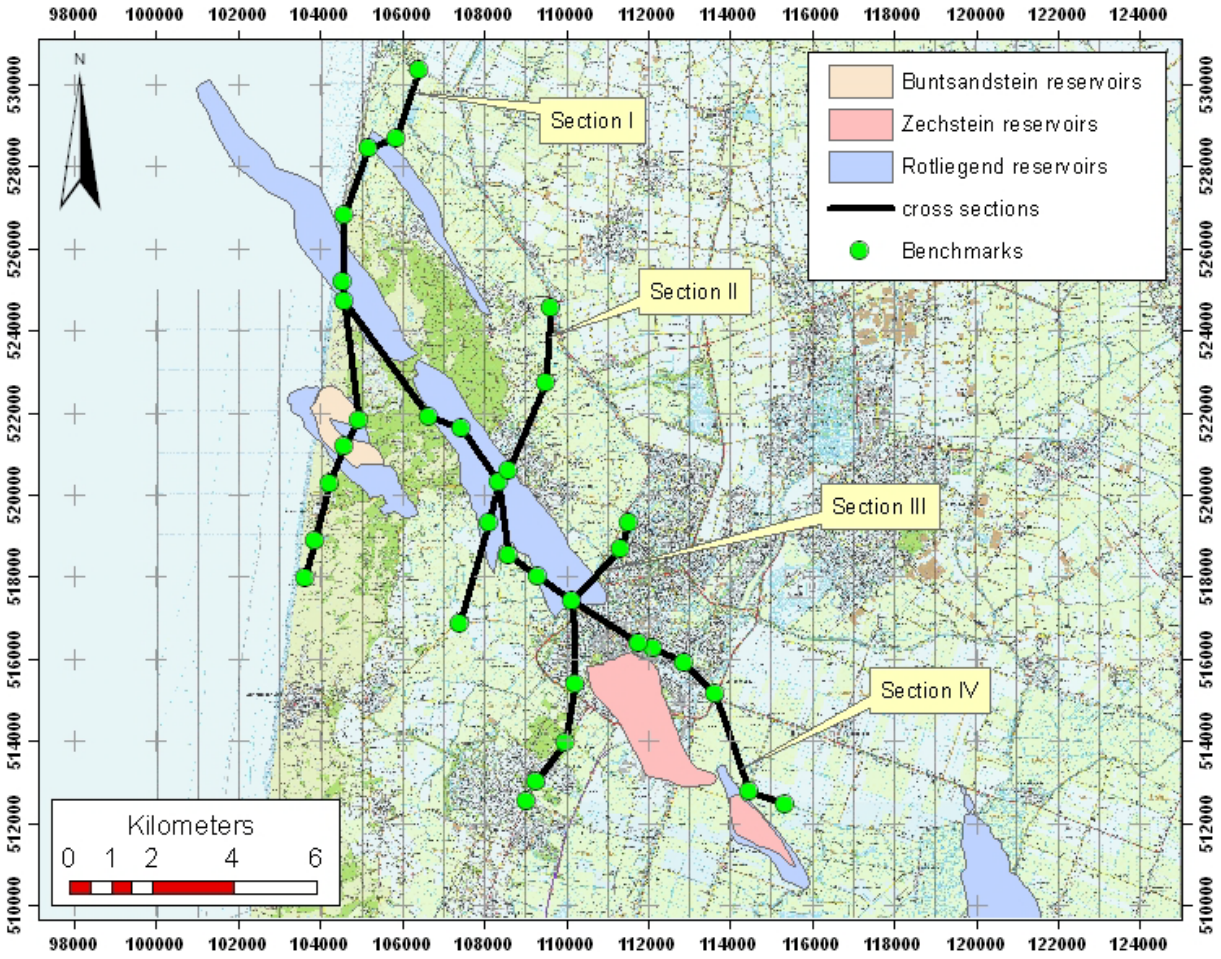

Figure 9: Location and paths of constructed cross sections and included benchmarks

All cross sections show a good fit across the area of interest, demonstrating that modelled values lie within the error of actual observed subsidence.

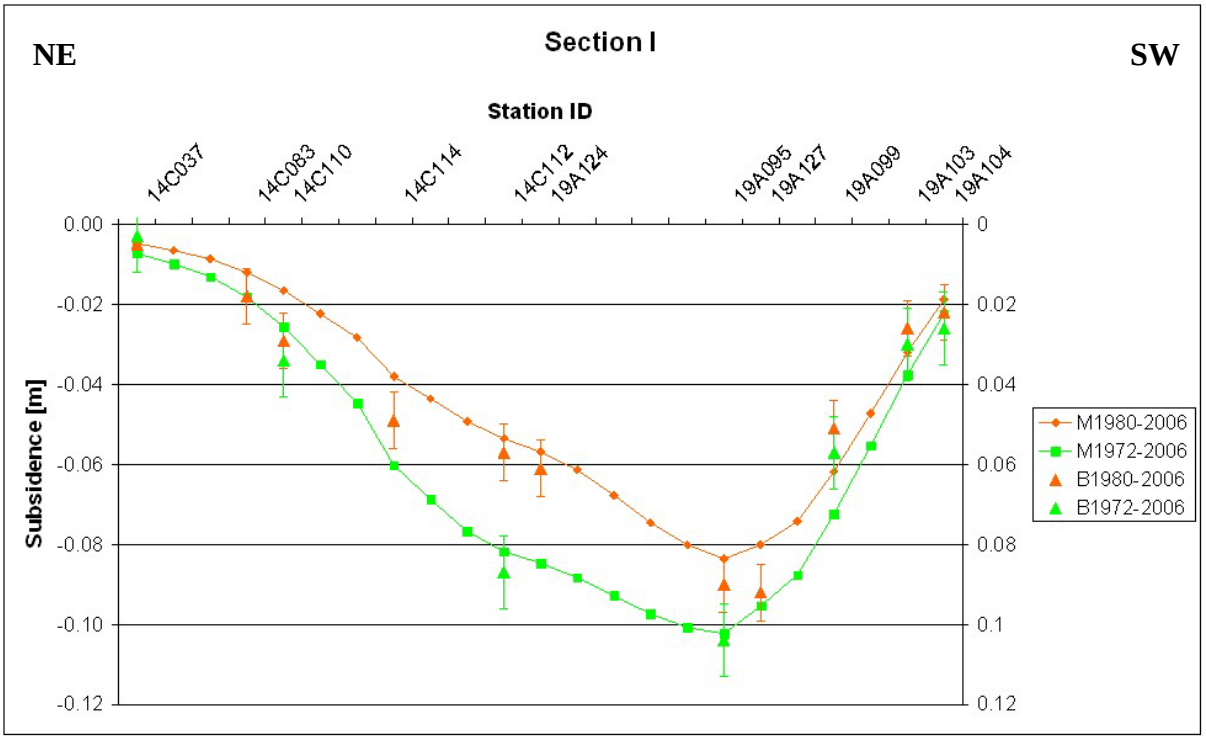

Figure 10: Cross section I location in Figure 9, displaying the modelled subsidence overlain by benchmark measurements

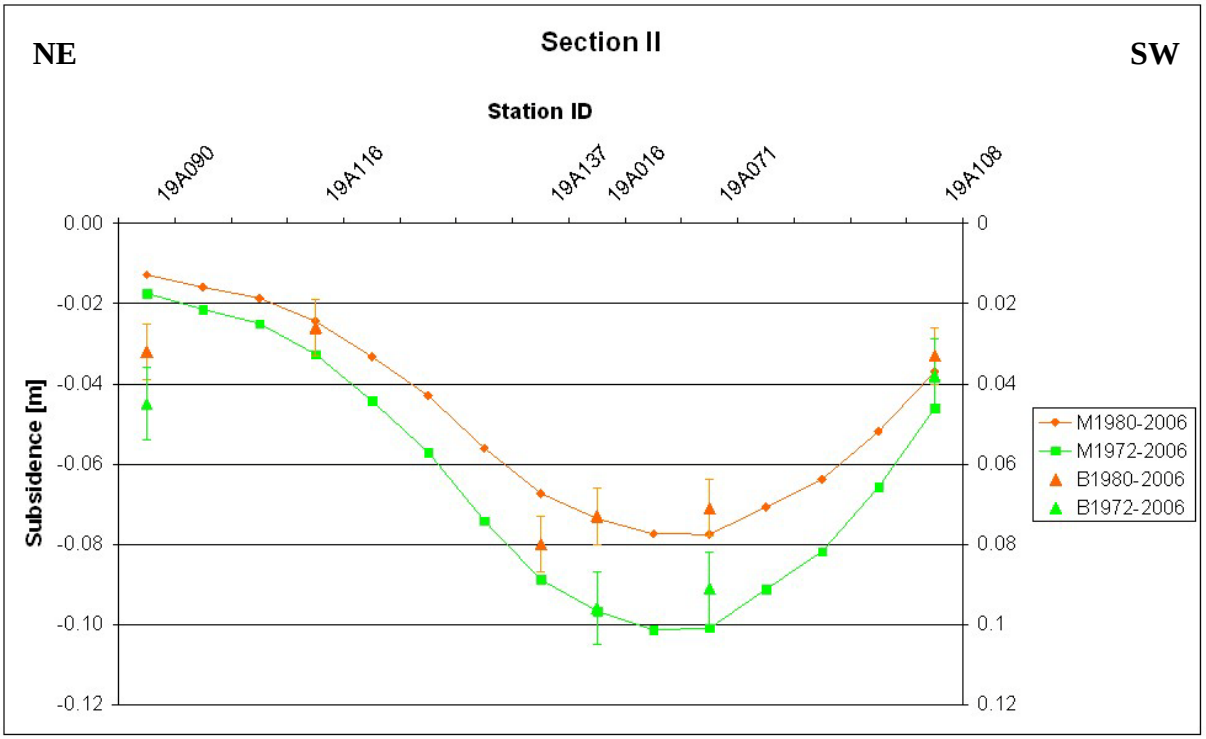

Figure 11:Cross section II location in Figure 9, displaying the modelled subsidence overlain by benchmark measurements

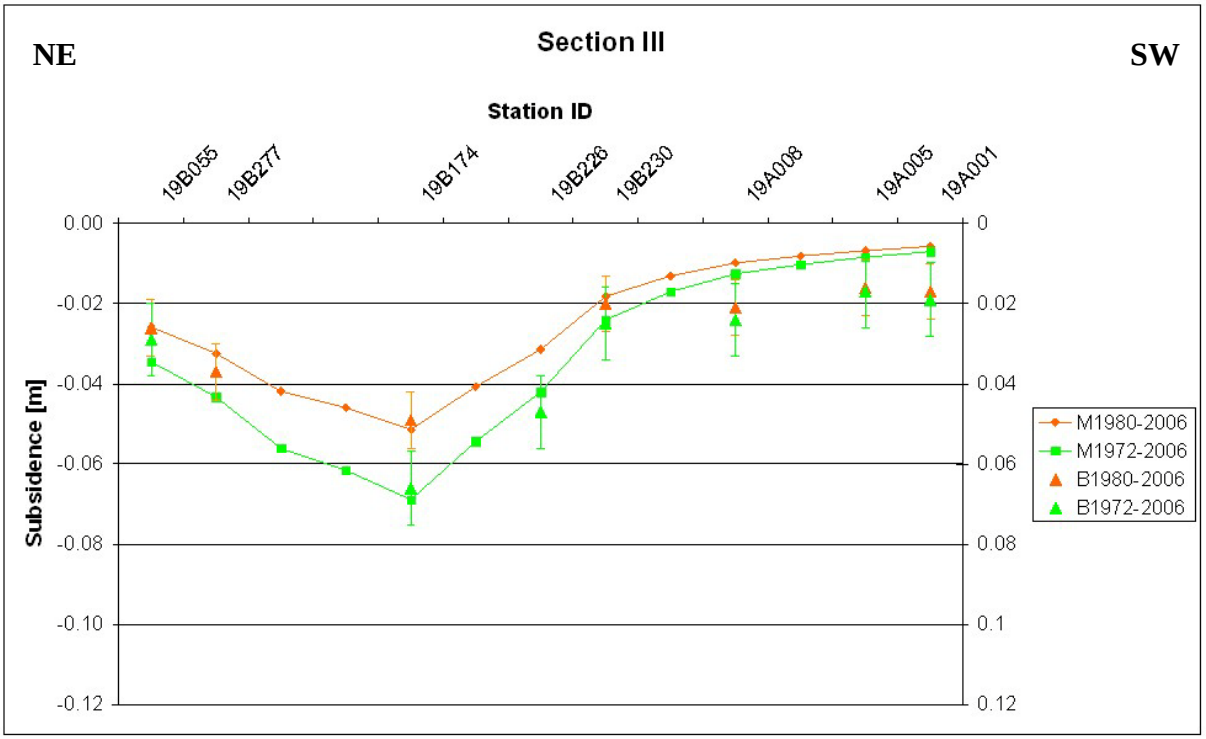

Figure 12: Cross section III location in Figure 9, displaying the modelled subsidence overlain by benchmark measurements

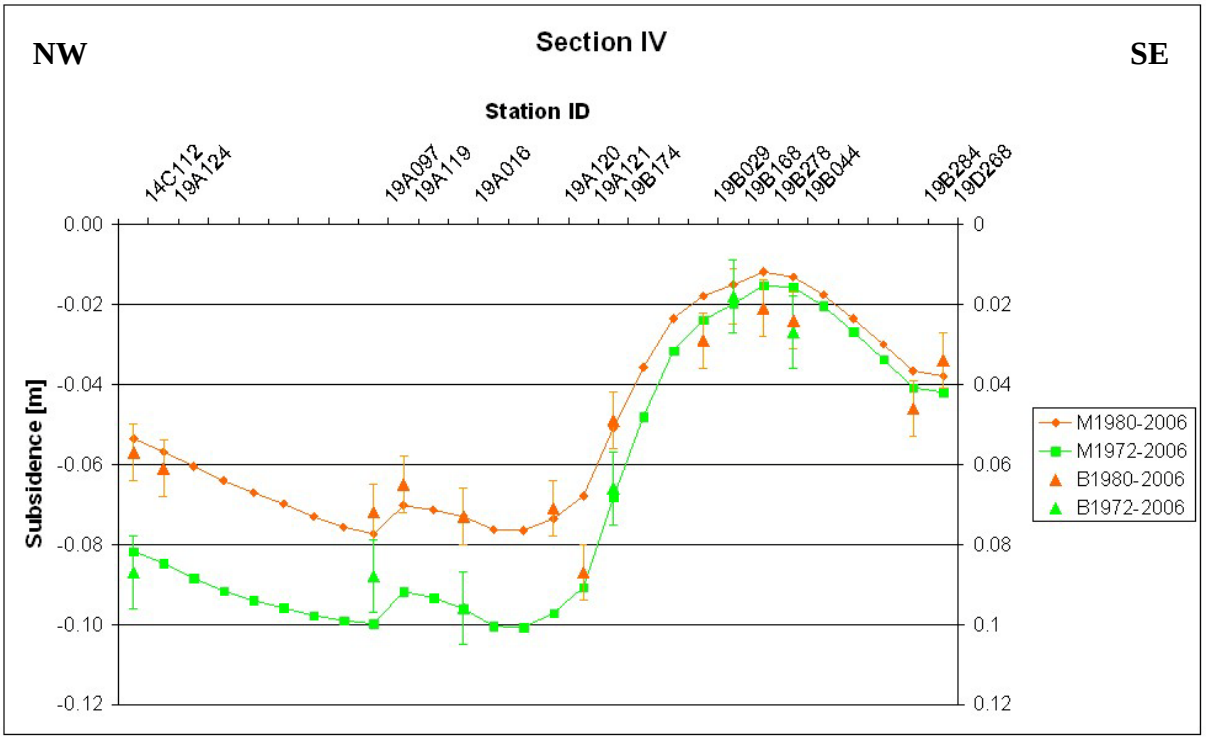

Figure 13: Cross section IV location in Figure 9, displaying the modelled subsidence overlain by benchmark measurements

3.1.5 Time series for selected benchmarks

The fit of the proposed model with actual benchmarks over the full time span from 1972 to 2006 was evaluated. To achieve this task, 6 out of 32 benchmarks that contain complete time series were selected at points above the main gas fields in the area of interest. Figure 14 gives an overview of available and selected benchmarks for analysis. The model was calculated for each time step contained in the benchmark data series (1972, 1980/81, 1984, 1988, 1991/92, 1997, 2001 and 2006) for each of the benchmark's locations. The evaluation was carried out by plotting the modelled and the measured subsidence over time. Figures 15 to 20 show these. The deviation of the modelled from the actual measured subsidence is hardly greater than 1 cm and mostly below 0.5 cm. Additionally all benchmarks containing complete time series were plotted against modelled values for each time step. Figure 21 shows that almost all data points for each time step lay within an error margin of 1 cm. The few out-lying points arise from 4 benchmarks only, and are marked in Figure 14. Two of these benchmarks are associated with the additional subsidence bowl described near the water treatment facility Geestmerambacht. One out-lying benchmark is located at the seawall, possibly associated with additional compaction due to heightening of the seawall.

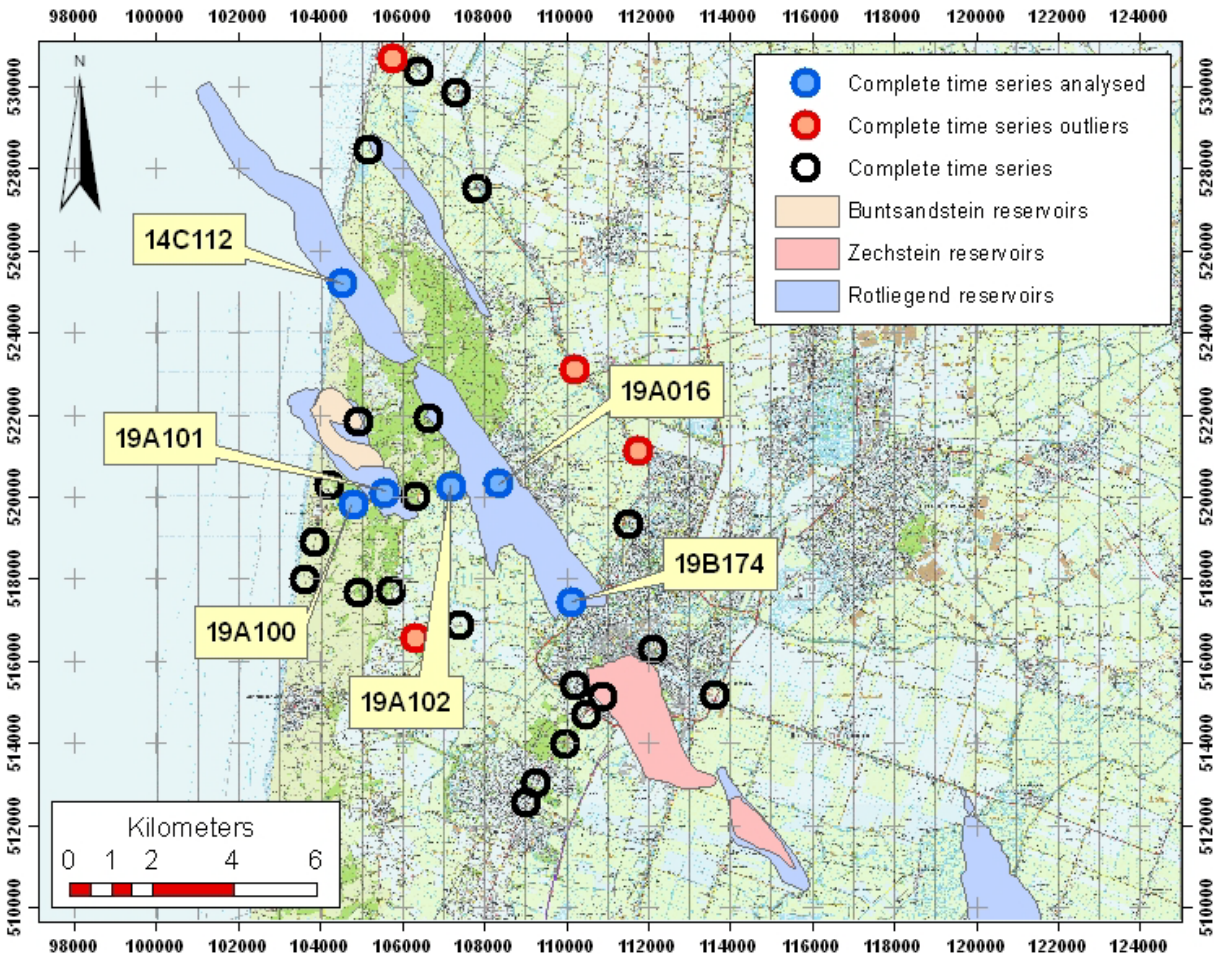

Figure 14: Benchmarks with complete time series available; analysed benchmarks are marked blue, benchmarks not lying on the general trend are marked as outliers in red

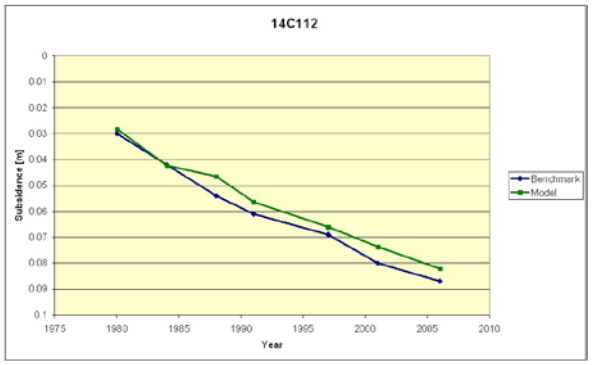

Figure 15: Time series for benchmark 14C112; modelled subsidence is shown in blue, measured in green

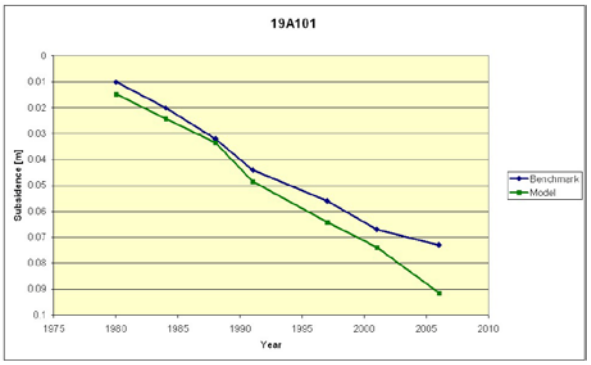

Figure 16: Time series for benchmark 19A101; modelled subsidence is shown in blue, measured in green

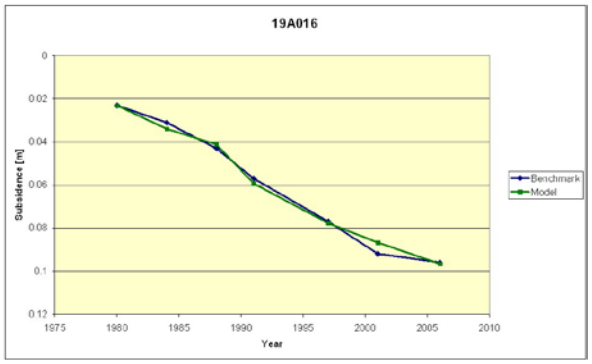

Figure 17: Time series for benchmark 19A016; modelled subsidence is shown in blue, measured in green

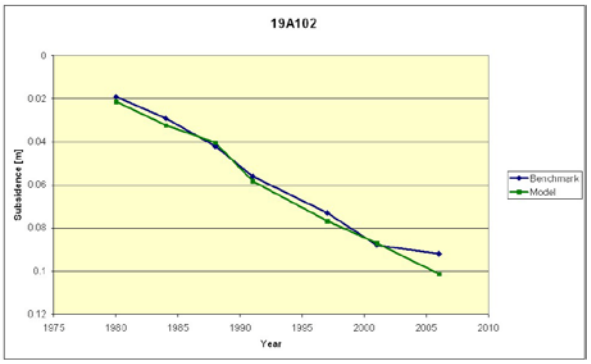

Figure 18: Time series for benchmark 19A102; modelled subsidence is shown in blue, measured in green

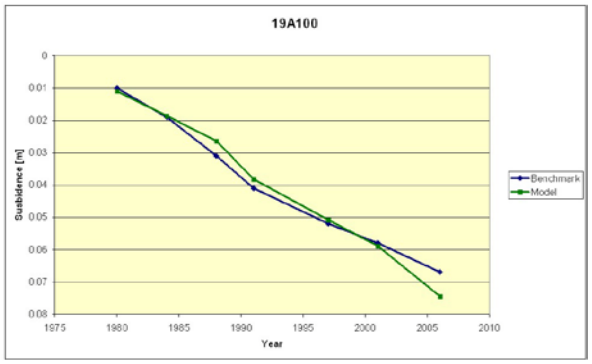

Figure 19: Time series for benchmark 19A100; modelled subsidence is shown in blue, measured in green

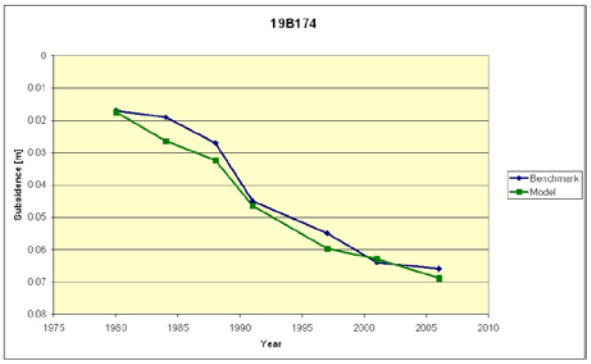

Figure 20: Time series for benchmark 14B174; modelled subsidence is shown in blue, measured in green

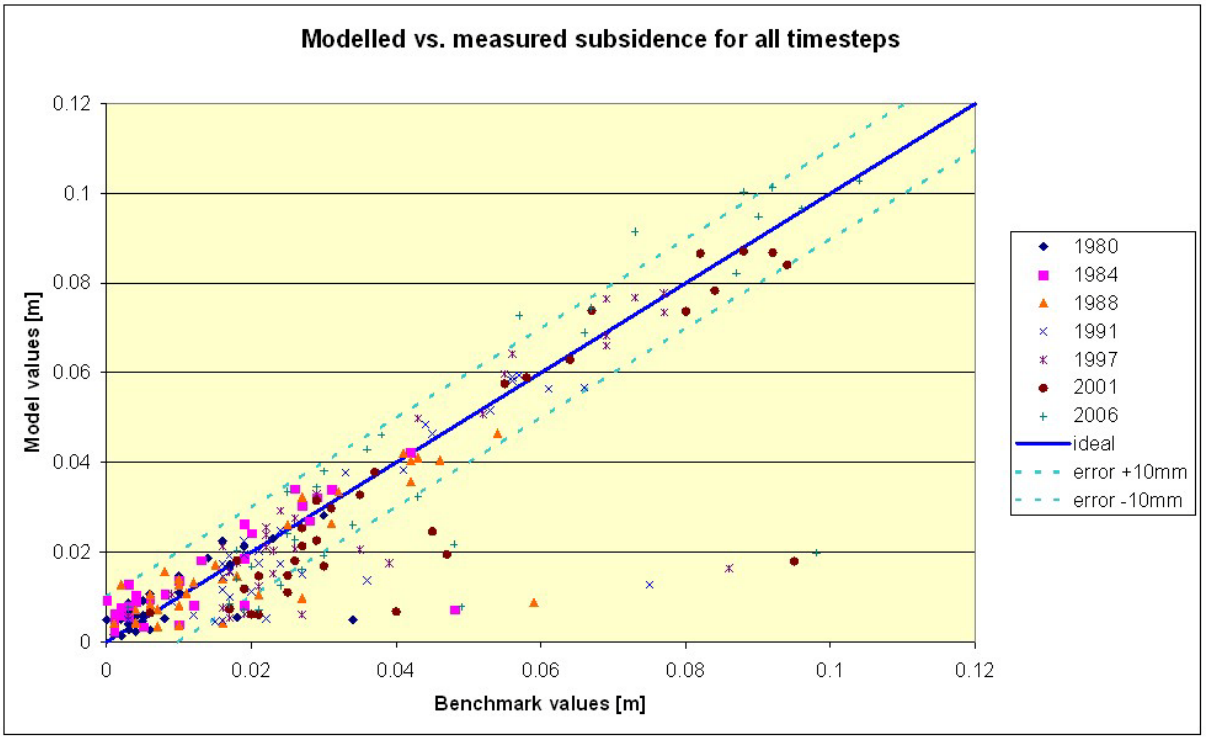

Figure 21: Modelled subsidence plotted versus measured subsidence at benchmarks for all timesteps. Outliers are associated with 4 benchmarks as outlined in Figure 14.

3.2 Subsidence prediction scenarios

3.2.1 Full depletion scenario

In order to calculate the maximum possible subsidence the field pressures have been reduced down to 10 bar, i.e. down to the maximum abandonment pressure. All models have been recalculated according to these assumptions. The Alkmaar field, reservoired in the Zechstein formation, is currently used for underground gas storage and actual pressures exceed initial pressures by up to ~ 10 bar. To predict the maximum subsidence at some time in the future, when it's gas storage function may cease, this field has been assumed to be completely depleted to the maximum abandonment pressure (10 bar).
The maximum calculated total subsidence was calculated according to the initial pressures from 1972. The center of the bowl is predicted to subside to a total of 12.1 cm with reference to the year 1972. The subsidence in the Westbeemster area is predicted to reach 8.6 cm at maximum. The subsidence bowl for the full depletion scenario is shown in appendix 5.1.5.

3.2.2 Storage scenario for Alkmaar and Bergermeer

In order to describe a future scenario, in which both the Alkmaar and the Bergermeer field will be used as underground gas storage, a second subsidence prediction model was calculated. Parameters from the maximum depletion scenario have been applied. Residual pressure during the post winter draw down phase in field Bergermeer was taken at 77 bar, as instructed by TAQA. For field Alkmaar the pressure declines observed in subsequent storage/extraction cycles have been taken, as it is already in use as gas storage.
In the centre of the subsidence bowl, a maximum of 11.0 cm is predicted. In this scenario the field Westbeemster will be depleted down to 10 bar as well, which results in a maximum of

8.6 cm subsidence as predicted in the full depletion scenario. The subsidence bowl for the storage scenario is shown in appendix 5.1.6.

3.2.3 Cross sections through predicted subsidence bowls

In order to assess the predicted scenarios, the full depletion and storage scenario was calculated along the lines I, II, III and IV (Figure 9, page 21). They were plotted on top of the full time span (1972 – 2006) model. Figure 22, Figure 23, Figure 24 and Figure 25 show cross-sections I, II, III and IV.

It is noticeable that the full depletion scenario is predicted to add additional subsidence of one to two cm in the whole area of interest. The storage scenario on the other hand predicts local uplift of up to 2.5 cm with reference to the year 2006.

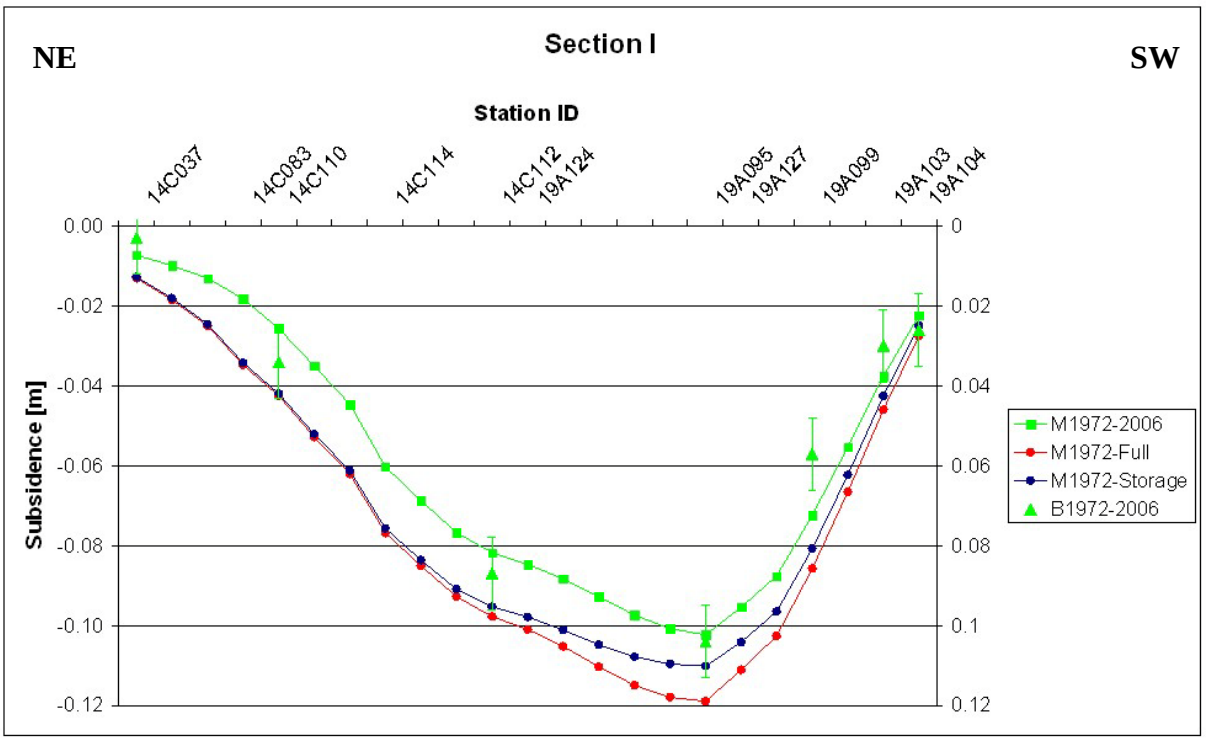

Figure 22: Cross section I location in Figure 9, displaying the modelled subsidence from 1972 - 2006 overlain by benchmark measurements. The predicted subsidence for the full depletion and the storage scenario are displayed additionally.

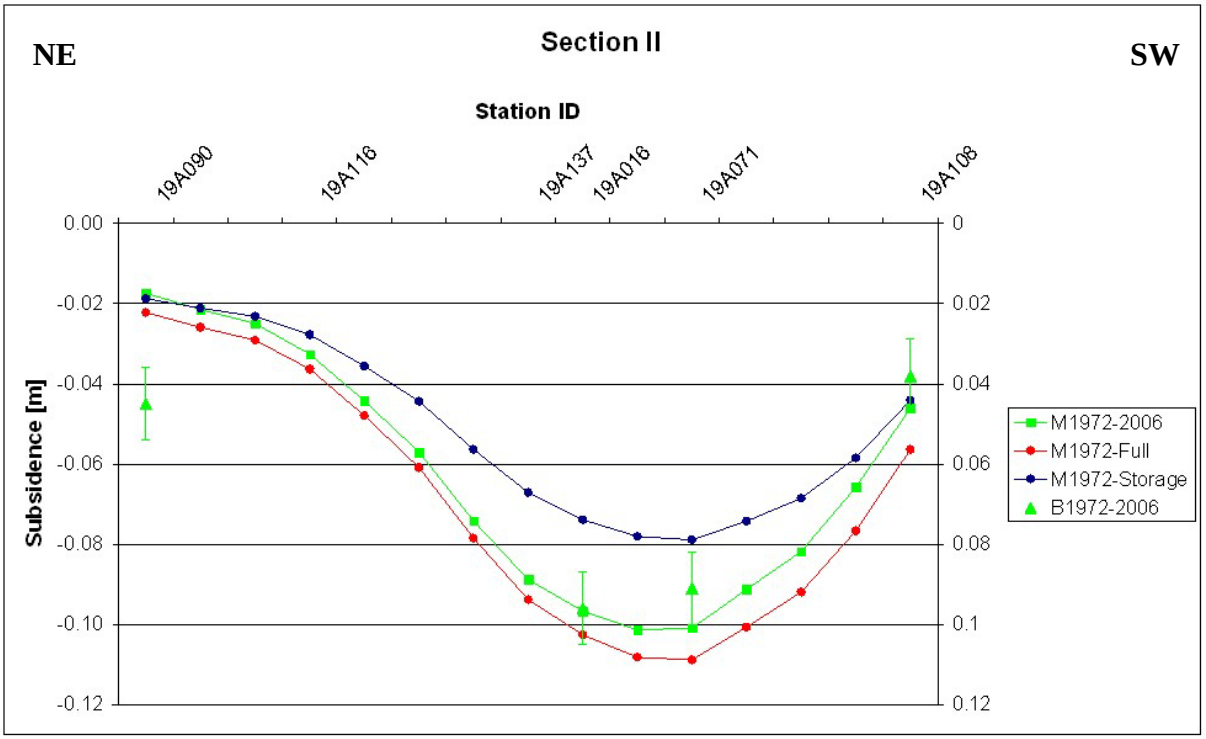

Figure 23: Cross section II location in Figure 9, displaying the modelled subsidence from 1972 - 2006 overlain by benchmark measurements. The predicted subsidence for the full depletion and the storage scenario are displayed in addition.

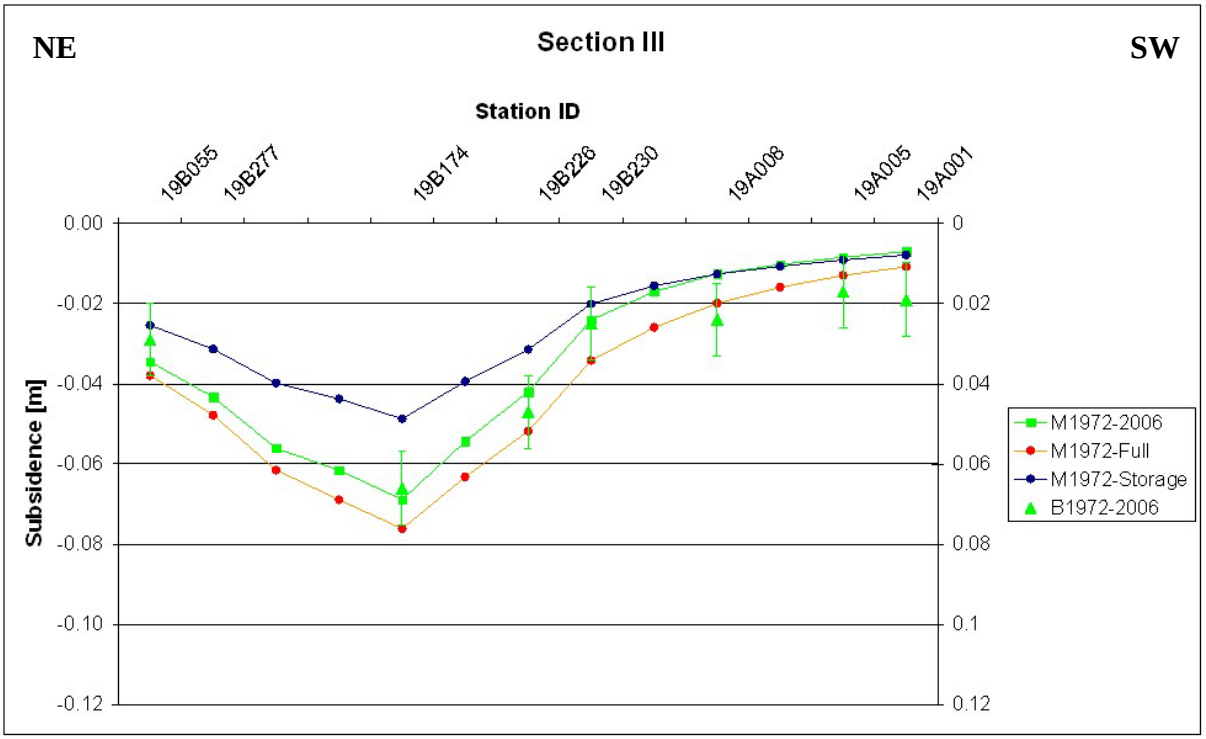

Figure 24: Cross section III location in Figure 9, displaying the modelled subsidence from 1972 - 2006 overlain by benchmark measurements. The predicted subsidence for the full depletion and the storage scenario are displayed in addition.

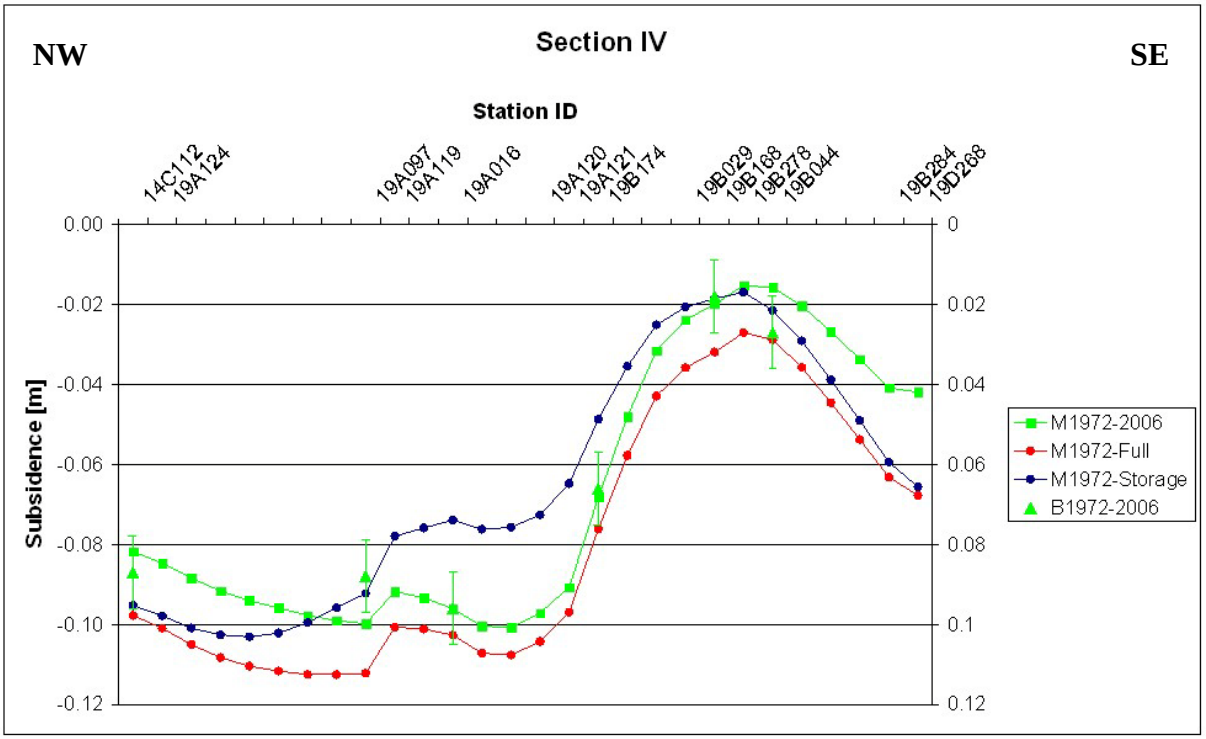

Figure 25: Cross section IV location in Figure 9, displaying the modelled subsidence from 1972 - 2006 overlain by benchmark measurements. The predicted subsidence for the full depletion and the storage scenario are displayed in addition.

3.2.4 Additional subsidence

In order to analyse the additional subsidence predicted after 2006, a differential bowl was calculated. For this, the subsidence bowl describing the 2006 situation was subtracted from the maximum depletion and the storage scenario bowl. The results are presented in Appendix 5.1.7 and 5.1.8.

The maps show that the strongest additional subsidence is predicted over the field Westbeemster. The second area where additional subsidence is expected is above the field Groet and Groet-Oost. Both scenarios, the full depletion and the storage scenario calculate the additional subsidence to occur in the same areas. Table 10 displays predicted total and additional maximum subsidence values in the described areas for each scenario.

Table 10: Maximum subsidence predicted per area and scenario

	Westbeemster		Groet	
	Full depletion scenario	Storage scenario	Full depletion scenario	Storage scenario
Subsidence from 1972 till 2006	0.6 cm	0.6 cm	10.0 cm	10.0 cm
Additional subsidence from 2006 onwards	8.0 cm	8.0 cm	2.1 cm	1.0 cm
Total subsidence since 1972	8.6 cm	8.6 cm	12.1 cm	11.0

4 CONCLUSIONS

- Pressure depletion data applied to a model of elastic reservoir compaction and propagation through overburden layers to the surface can successfully be used in a model to calculate subsidence, which matches observed surface subsidence, and to predict future subsidence.
- Pressure decline is assumed to occur in the gas reservoirs as well as in their connected aquifers. P/Z data show no pressure support from dynamic aquifers, supporting the assumption of a limited extent of the aquifers.
- Cumulative production versus subsidence plots support the general observation of bilinear compaction of the Rotliegend in this area, resulting in two compaction coefficients applied.
- Modelled subsidence data for the period from 1972 to 2006 align closely with actual measured subsidence data, validating the model used to predict future subsidence.
- Additional subsidence from 2006 until full depletion is predicted to be 8.0 cm in the Westbeemster area, and 2.1 cm in the Groet / Groet-Oost area.
- The storage scenario, in which both fields Alkmaar and Bergermeer will be used as UGS (Underground Gas Storage facility), predicts an additional subsidence of 1.0 cm occurring during the economic life of the storage facilities from 2006 onwards in the Groet / Groet-Oost area. The maximum subsidence predicted in the full depletion scenario would not be different in the storage scenario for the Westbeemster area.
- The storage scenario predicts an uplift of up to 2.5 cm in the Bergermeer area due to gas injection into the previously depleted reservoir.

References

Fokker, P.A. & Orlic, B., 2006. Semi-analytic modelling of subsidence. Math. Geol. 38, 565-589.

Houtenbos, A.P.E.M., 2008. Bodemdalingsanalyse: Bergen-Alkmaar 1972-2006

Muntendam-Bos et al., 2008. Bergermeer Seismicity Study. TNO report 2008-U-R0871/B

5 APPENDIX

Subsidence modelling was done with AEsubs – Version 5.1 Beta – March 2008

Contours have been calculated from point data sets using Halliburton Geographix 5.0.0.1.

All maps have been produced using ESRI ArcGIS 9.3.1

5.1 Maps

5.1.1 Model input data

This map presents an overview of all input data included. The outline of included fields and all subsidence field measurements available are marked. Rotliegend aquifers are presented semi-transparent.
Map format is A3; stored in *Appendix_5.1.1.pdf*

5.1.2 Subsidence from 1972 to 1980/81, modelled and measured

This map shows the results of the subsidence modelling from 1972 to 1980/81. Displayed circles represent field measurement values.
Map format is A3; stored in *Appendix_5.1.2.pdf*

5.1.3 Subsidence from 1980/81 to 2006, modelled and measured

This map shows the results of the subsidence modelling from 1981/81 to 2006. Displayed circles represent field measurement values.
Map format is A3; stored in *Appendix_5.1.3.pdf*

5.1.4 Subsidence from 1972 to 2006, modelled and measured

This map shows the results of the subsidence modelling from 1972 to 2006. Displayed circles represent field measurement values.
Map format is A3; stored in *Appendix_5.1.4.pdf*

5.1.5 Total subsidence – Full depletion scenario

This map displays the total subsidence predicted in the full depletion scenario. Map format is A3; stored in *Appendix_5.1.5.pdf*

5.1.6 Total subsidence – Storage scenario

This map displays the total subsidence predicted in the storage depletion scenario. Map format is A3; stored in *Appendix_5.1.6.pdf*

5.1.7 Additional subsidence – Full depletion scenario

This map displays the difference of the total subsidence predicted in the full depletion scenario and the total subsidence modelled till 2006. It shows all additional subsidence predicted from 2006 on.
Map format is A3; stored in *Appendix_5.1.7.pdf*

5.1.8 Additional subsidence – Storage scenario

This map displays the difference of the total subsidence predicted in the storage scenario and the total subsidence modelled till 2006. It shows all additional subsidence predicted from 2006 on.
Map format is A3; stored in *Appendix_5.1.8.pdf*